Table S1

List of primary and secondary antibodies

Antigen [Antibody clone]	Provider	IHC dilution	IF dilution
PRIMARY ANTIBODIES			
CD3	Novocastra, Newcastle upon Tyne, United Kingdom	1:100	
CD20 [L26]	DAKO, Copenhagen, Denmark	1:1000	
CD31 [JC70A]	DAKO, Copenhagen, Denmark	1:50	
CD45RO [UCHL1]	DAKO, Copenhagen, Denmark	1:200	
CD63 [NK1/C3]	Abcam, Cambridge, United Kingdom	1:100	1:50
CD68 [PGM1]	DAKO, Copenhagen, Denmark	1:200	
LAMP1 [rabbit polyclonal]	kindly provided by Dr. S. Carlsson (University of Umea, Sweden)	1:10000	
Vimentin [V9]	BioGenex, Fremont, CA, USA	1:400	
S100 protein [rabbit polyclonal]	DAKO, Copenhagen, Denmark	1:10000	
CD1a [rabbit monoclonal, EP3622]	ZYTOMED, Berlin, Germany	1:500	
Langerin [rabbit monoclonal, EPR15863]	Abcam, Cambridge, United Kingdom	1:200	
smooth muscle (sm) actin [1A4]	DAKO, Copenhagen, Denmark	1:200	
Desmin [D33]	DAKO, Copenhagen, Denmark	1:200	
LAMP2 [goat polyclonal]	R&D Systems, Minneapolis, MN, USA		1:50
CD68 [rabbit monoclonal, EPR20545]	Abcam, Cambridge, United Kingdom		1:1000
SECONDARY ANTIBODIES			
[Donkey] anti-Goat AF568 IgG	Invitrogen – Thermo Fisher Scientific (Carslbad, CA, USA)		1:500
[Donkey] anti-Mouse AF488 IgG	Invitrogen – Thermo Fisher Scientific (Carslbad, CA, USA)		1:500
[Donkey] Anti-Rabbit AF555 IgG	Invitrogen – Thermo Fisher Scientific (Carslbad, CA, USA)		1:500
[Donkey] Anti-Goat AF647 IgG	Invitrogen – Thermo Fisher Scientific (Carslbad, CA, USA)		1:500

Fig. S1

Adenotonsillar pathology in an untreated MPS I patient (#3)

(**a**) anti-CD3 and (**b**) anti-CD20 staining. (**c**, **d**) CD68+ macrophages predominate in follicular germinal centers (outlined by dashed line). Image shown in **d** corresponds to the rectangle (in the paracortex) in **c**; (**e**, **f**) vacuolated CD63+ cells populate paracortex. Image in **f** corresponds to the rectangle in **e**. **a** - **f** images originate from serial histological sections; (**g**) cytoplasm of follicular germinal center macrophages contains pleoimorphic vacuoles (black arrows); (**h, i**) paracortical cells contain partly cleared membrane-bound storage vacuoles with fine granular contents.

scale bars = 100 μm (**a**, **b**, **c**, **e**); 2 μm (**g-i**)

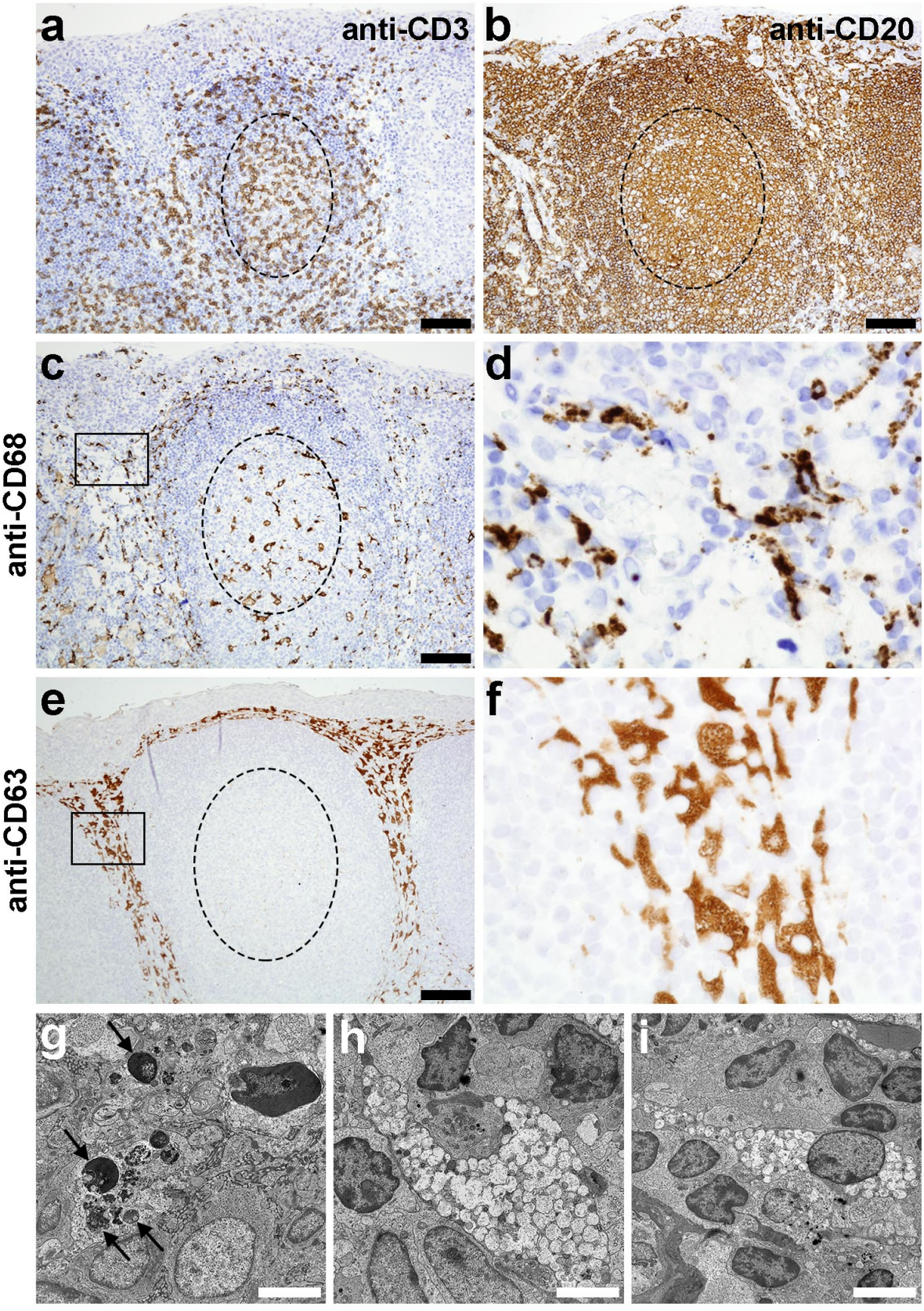
a
anti-CD3
b
anti-CD20
c
d
anti-CD68
e
f
anti-CD63
g
h
i

Fig. S2

Comparison of IHC staining patterns of CD63 and CD68 with S-100, CD1a, Langerin, desmin, vimentin, and smooth muscle (sm) actin in an MPS II patient (#4).

(**a**) anti-CD63, (**b**) anti-CD68, (**c**) anti-S100, (**d**) anti-CD1a, (**e**) anti-langerin, (**f**) anti-desmin, (**g**) anti-vimentin, and (**h**) anti-sm-actin. Images from serial sections are shown.

scale bars = 100 μm (**a**-**d**); *representative images are shown*

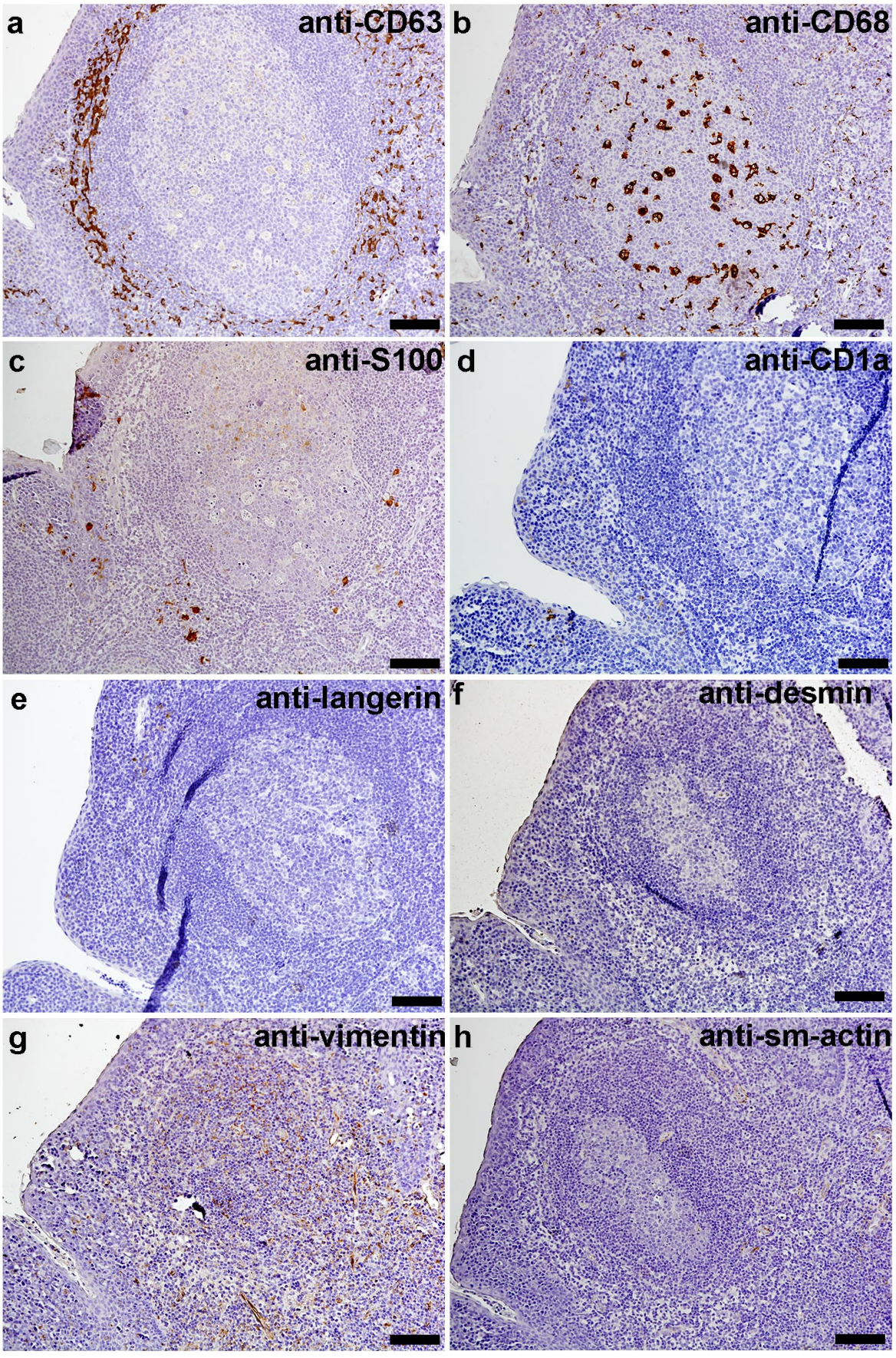
a
anti-CD63
b
anti-CD68
c
anti-S100
d
anti-CD1a
e
anti-langerin
f
anti-desmin
g
anti-vimentin
h
anti-sm-actin

Fig. S3

Adenotonsillar findings in HSCT and ERT treated MPS I patients.

Adenoidectomy was performed 4 years and 4 months after HSCT (patient #1) and 7 months after initiation of ERT (patient #2).

(**a**-**d**) the number of CD68+ and CD63+ cell is substantially lower compared to a patient who was not treated at the time of adenoidectomy (*Fig. S1*). Distribution of CD68+ and CD63+ cells is comparable to control tissues (*Fig. S3*). Dashed lines and black arrows highlight the germinal centers and epithelial surface, respectively. Images from serial sections are shown for both patients.

Nonspecific histopathological inflammatory changes were comparable to findings in non-MPS/non-LS controls.

scale bars = 100 μm (**a**-**d**); *representative images are shown*

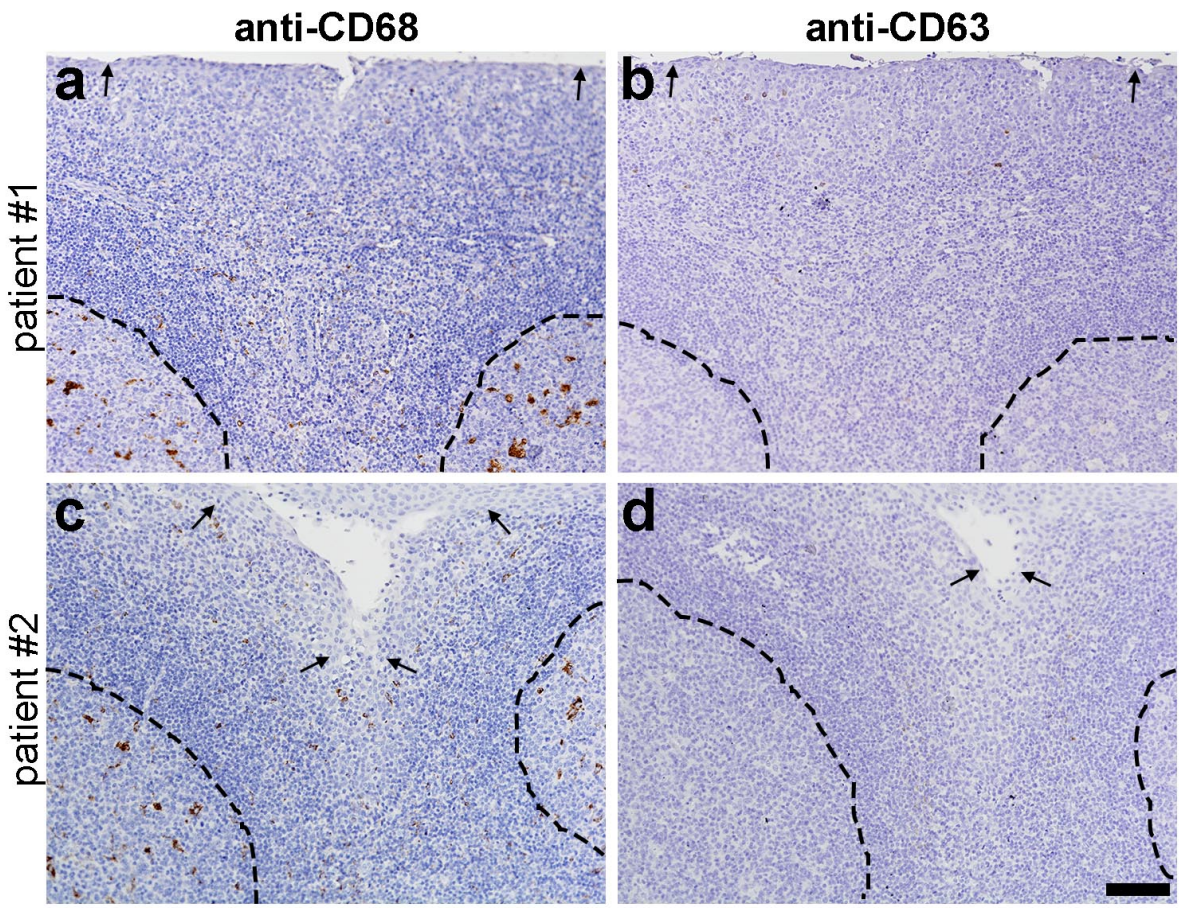
anti-CD68
anti-CD63
a
b
c
d
patient #1
patient #2

Fig. S4

CD68 and CD63 expression in non-MPS/non-LS adenotonsillar tissue.

Tissue samples from all non-MPS/non-LS controls shared similar nonspecific histopathological inflammatory changes corresponding to findings commonly associated with the clinical diagnosis of adenotonsillar hypertrophy. Lymphoid tissues were covered by locally eroded pseudostratified ciliary respiratory and/or squamous epithelium. Lymphoid germinal centers were hyperplastic and with abundant vacuolated histiocytes/macrophages. (**a**, **c**, **e**) CD68+ cells are almost exclusively restricted to follicular germinal centers (outlined by dashed lines). (**b**, **d**, **f**) Paracortical areas do not contain CD63+ cells. CD63+ cells are seen scattered in the medullary sinuses/cords.

Black arrows (**a**, **c**) highlight epithelial surface. Areas outlined by the rectangles in **c** and **d** correspond to images shown as **e** and **f**, respectively. Images from serial histological sections are shown for both immunohistochemical stains.

scale bars = 100 μm (**a**, **b**, **e**, **f**); 200 μm (c, d); *representative images are shown*

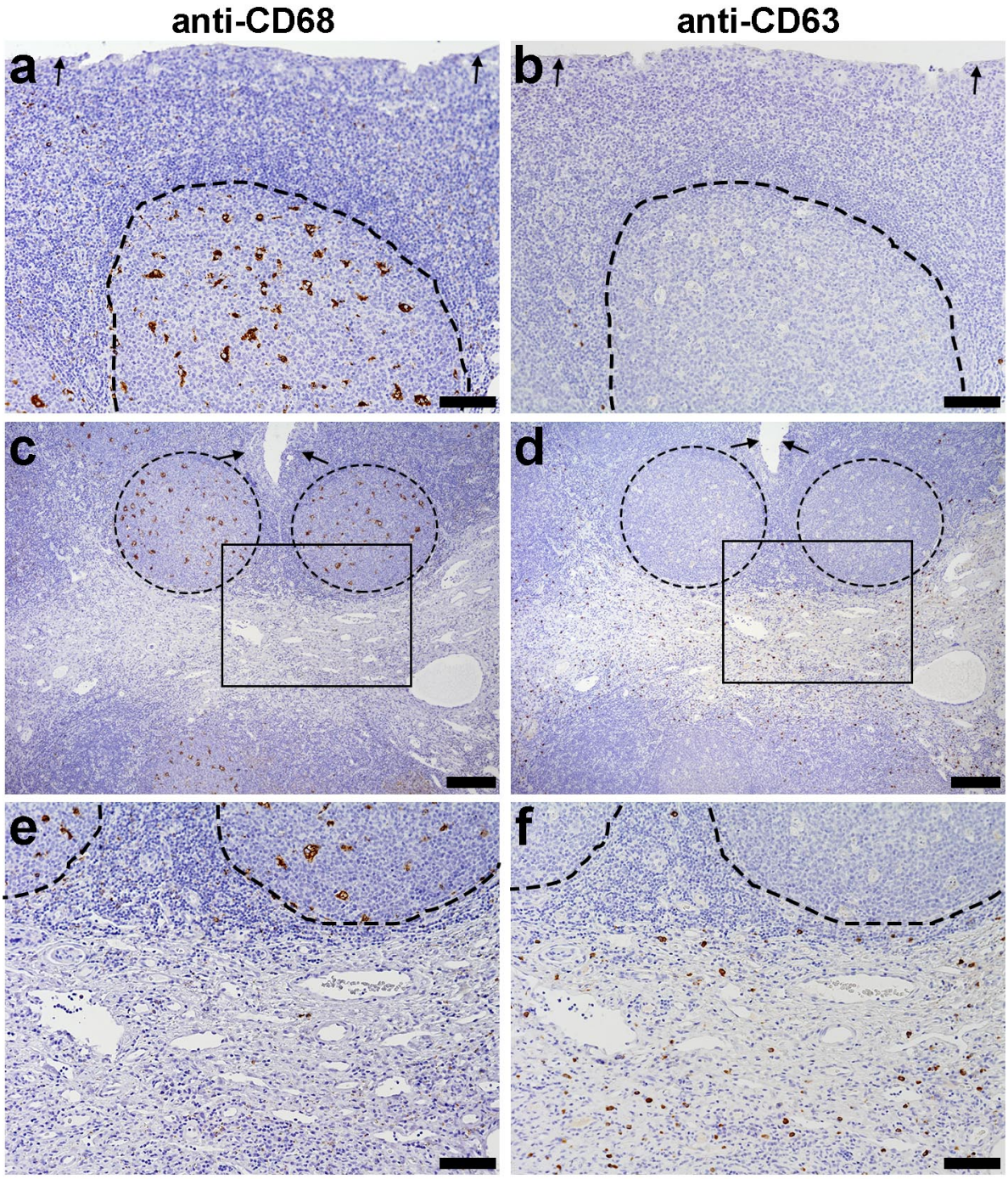
anti-CD68
anti-CD63
a
b
c
d
e
f

Fig. S5

CD63 expression in storage lysosomes of non-lymphoid tissues in MPS patients.

(**a-d**) MPS IIIA patient (*SGSH* (NM_000199.5): c.[250-2A>G];[703G>A], p.[His84_Gln85del];[Asp235Asn])

(**e**) MPS II patient (*IDS* (NM_000202.8): c.[1212_1215dup];[0], p.Leu406ValfsTer26)

(**f**) MPS VII patient (*Marek et al.* (2021) Cardiovasc. Pathol.)

(**a**) cerebellar cortex, Purkinje cells bodies (black arrows), storage lysosomes in Purkinje cells dendrites (white arrows) are CD63+; (**b**) brain stem neurons with CD63+ storage lysosomes; (**c**) CD63+ storage lysosomes in the chondrocytes of the tracheal cartilage; (**d**) valvular intersticial cells (VICs) of the aortic valve with CD63+ storage lysosomes; (**e**) CD63+ lysosomes in cortical neurons; (**f**) valvular intersticial cells (VICs) of the aortic valve with CD63+ storage lysosomes.

scale bars = 50 μm

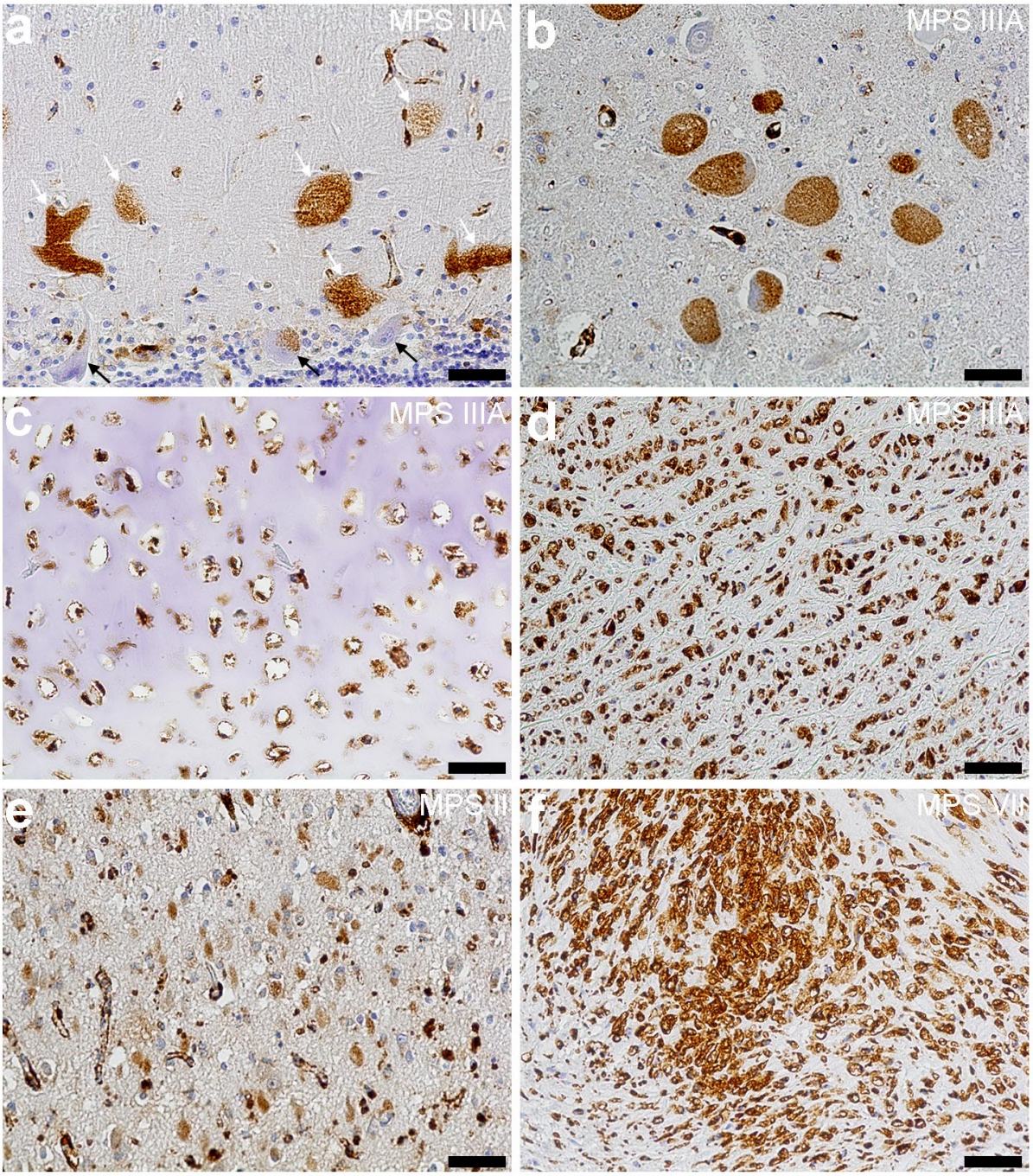
a
MPS IIIA
b
MPS IIIA
c
MPS IIIA
d
MPS IIIA
e
MPS II
f
MPS VII

Fig. S6

Adenotonsillar pathology in a patient with infantile neurovisceral variant of ASM deficiency.

(**a**, **b**) CD68+ cells cluster in the tissue and are not restricted to germinal centers (outlined by dashed lines) as in MPS patients. CD68+ cells can be found in paracortical areas and sinuses. (**c**, **d**) CD63+ cells are present in the paracortical areas in larger numbers than in control non-MPS tissues, but are not vacuolated. CD63 can also be detected in areas populated by clustered CD68+ cells.

Areas outlined by the rectangles in **a** and **c** correspond to images shown as **b** and **d**, respectively.

Images from serial sections are shown for both immunohistochemical stains.

scale bars = 200 μm (**a**, **c**); 20 μm (**b**, **d**)

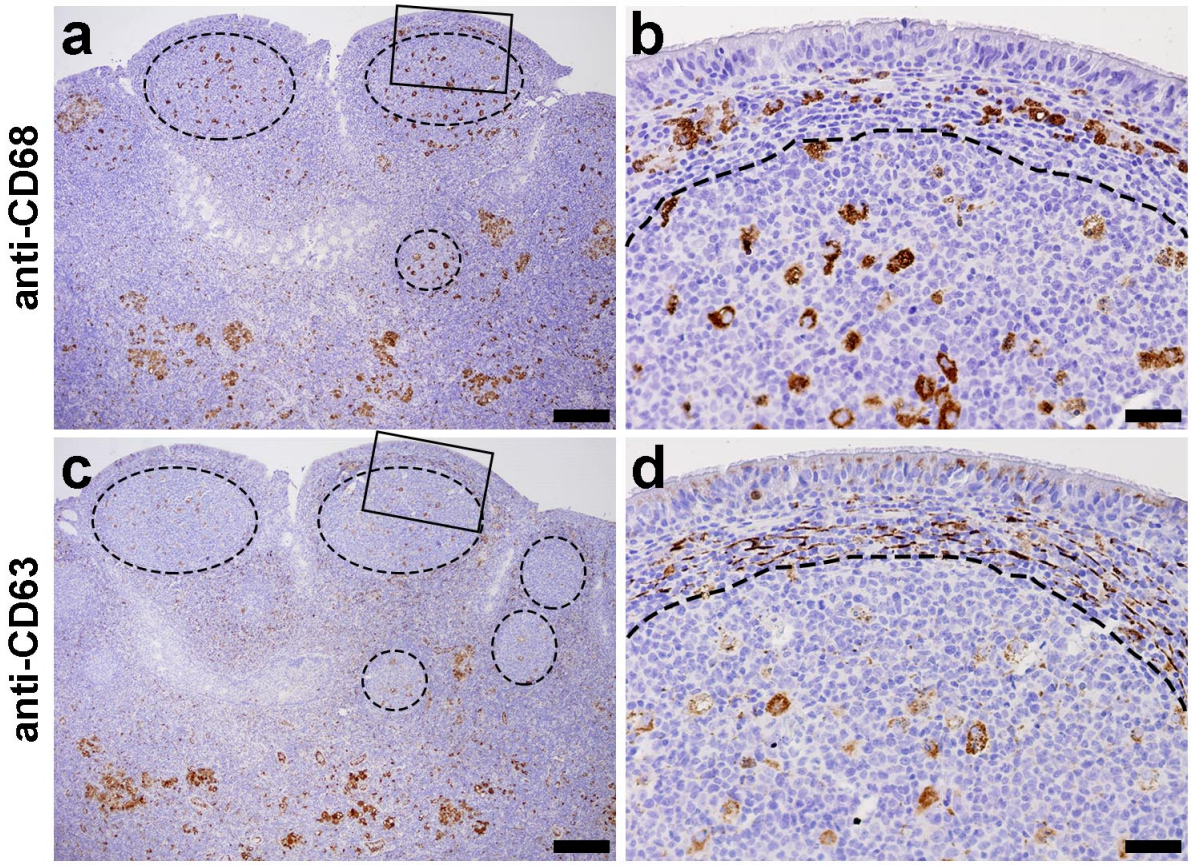
a
b
c
d
anti-CD68
anti-CD63

Fig. S7

Distribution of CD63+ and CD68+ lysosomes in adenotonsillar tissue of a patient with infantile neurovisceral variant of ASM deficiency.

Tissue sections were triple-stained with anti-CD63, anti-CD68, and anti-LAMP2 primary antibodies and detected by fluorescently labeled species-specific secondary antibodies (*Tab. S1*).

(**a**) Germinal center (GC, outlined by dotted line) and paracortex. Region of interest #1 (ROI #1) shows part of GC and paracortex in detail.

GC macrophages (empty arrows) as well as macrophages of the paracortex (empty arrowheads) contain CD68+/CD63+ lysosomes (LAMP2+). Similar to adenotonsillar tissues of MPS patients, a population of paracortical cells (two highlighted by white arrows) contains excess of CD63+/LAMP2+ lysosomes. The storage pathology in these cells is morphologically less pronounced than in MPS patients.

(**b**) Storage-ladden macrophages cluster in lymphoid sinus areas of the adenotonsillar tissues. Lysosomes in these cells are CD63+/CD68+/LAMP2+.

Compare to Figures 1, 2, and *S5*.

scale bars = 20 μm

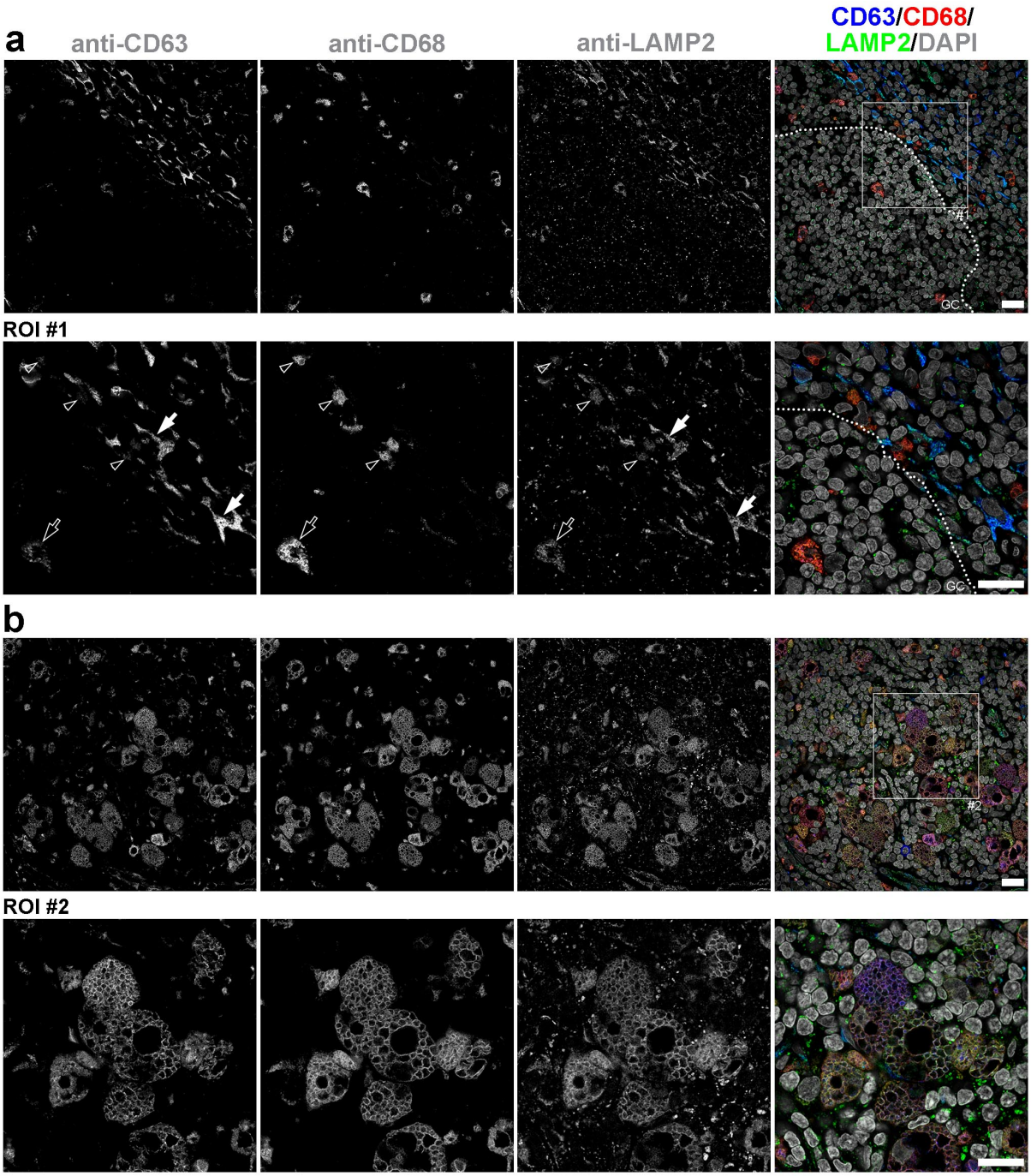
a
anti-CD63
anti-CD68
anti-LAMP2
CD63/CD68/
LAMP2/DAPI
#1
GC
ROI #1
GC
b
#2
ROI #2